Proceedings of the ICBBG2025
2025 International conference on Biomediated and Bioinspired Geotechnics
18-20 May, 2025 | Tempe, Arizona, USA
https://doi.org/10.53243/ICBBG2025-41

Methodology to generate root analogues based on root tensile behaviour

Shanshan Li, M.Sc.[1] and **Prof. Dr.-Ing., Hans H. Stutz**[2]

[1]Institute of Soil Mechanics and Rock Mechanics, Karlsruhe Institute of Technology, Engler-Bunte-Ring 14, 76131 Karlsruhe, Germany; E-mail: shan-shan.li@kit.edu
[2]Institute of Soil Mechanics and Rock Mechanics, Karlsruhe Institute of Technology, Engler-Bunte-Ring 14, 76131 Karlsruhe, Germany; E-mail: hans.stutz@kit.edu

ABSTRACT

Root mechanical properties and geometry are crucial for predicting root-soil mechanical reinforcement. However, in terms of natural roots, the high variability challenges the repeatability of root-soil experiments for determining the key factors influencing root reinforcement. This work aims to understand the tensile behaviour of individual roots, and develop root analogues based on the tension properties for parametric studies of soil-root interactions. The experimental results indicated that under uniaxial tension loading, three typical stress-strain curves can be identified, corresponding to different tension behaviours. This variability in response can be attributed primarily to the mechanical properties of the root stele, as well as to the integrity of the bonding between the stele and cortex. Additionally, the reproducible root analogues were developed using 3D printing techniques based on the tension properties of willow (*Salix purpurea* L.) roots. Our preliminary tests demonstrated that resin-based prints fabricated with Stereolithography Apparatus (SLA) technology exhibited a great potential to simulate real willow roots. The development of such analogues is expected to yield useful insights for optimizing engineered plant root systems in slope stabilization.

INTRODUCTION

Plants offer an effective and environmentally friendly approach to enhancing resistance to soil erosion and landslides (Martinez et al. 2022). Mechanical properties of plant roots (e.g., tensile strength and stiffness) are important parameters for quantifying plant anchorage or its contribution to reinforce soils. Most root biomechanical studies have reported results for tensile strength at breakage alongside the Young's modulus, indicating that they were influenced by root diameter, length, moisture, species, chemical composition, age, anatomy, as well as tensile test conditions (Li et al. 2023). However, research on root stress-strain behaviour is comparatively limited. Several studies have identified non-linear root tensile behaviour, typically occurring in two phases: an elastic phase with relatively high stiffness, followed by a inelastic phase where stiffness decreases until ultimate tensile failure (Boldrin et al. 2018; Wu et al. 2024).

There have been a body of experimental studies performed on natural rooted soil to quantify root-soil interaction. However, the mechanics and architecture of natural roots are extremely variable due to environmental and genetic factors, posing challenges to the repeatability of related experiments. A few studies have employed root analogues constructed from materials such as wood

(Sonnenberg et al. 2012), rubber (Mickovski et al. 2007), aluminum (Ali et al. 2013), cable(Wu et al. 1988), and cotton (Schwarz et al. 2011) to mimic simplified root structures, including tap root, herringbone, and dichotomous patterns. For more complex structures, 3D printing filaments have been used, e.g., ABS (Liang et al. 2017), PLA (Chen et al. 2019) and TPU (Kim et al. 2024). These root analogues allowed researchers to specify their geometry, mechanical properties and spatial distribution. Nonetheless, there have been limited systematic comparisons of the mechanical properties between natural and artificial roots.

In geotechnical engineering, pioneer species like *Salix spp.*, are often preferred due to their swift propagation and high surviving rates in extreme environment (Fleischer et al. 2021). In this study, the stress-strain behaviour of natural roots (*Salix purpurea* L.) will be investigated with uniaxial tension tests. Furthermore, this work will present a resin-based root analogue to more realistically mirror tensile behaviour of willow individual roots.

MATERIALS AND METHOD

Plant roots. The species selected for this study is *Salix purpurea* L. (hereafter *S. purpurea*). Recognized for its shrub-like growth form, *S. purpurea* is deemed particularly suitable for willow brush mattresses in the riverbank construction due to its robust and flexible characteristics. The tested roots were sampled from Federal Waterways Engineering and Research Institute (BAW). To maintain root mechanical properties after sampling, roots were put into a 15% alcohol solution to prevent microbial degradation (Giadrossich et al. 2017).

Mechanical tests. Root mechanical properties were characterized by performing uniaxial tension tests (UT). To this end, we constructed a tension tester based on a conventional direct shear apparatus (Wykeham Farrance Engineering Ltd., U.K.). The tester was equipped with loading system, data acquisition system, and clamping system. During each test, the data acquisition system recorded the load (F [N]) and displacement (Δl [mm]) as a continuous curve, capturing data at a rate of 50 points per second. The motor loading velocity was kept constant to 1.22 mm/min, which is within the typical speed range in other studies (Li et al. 2023). To prevent roots slipping from clamps and to minimize damage to root ends, the ends were strengthened by glue and tapes. Root samples were pre-soaked in water for a few hours before testing. The dimensions of root samples were measured with a digital calipers. The initial gauge length (GL, distance between two clamps) was 10 cm. Three root diameters were measured, i.e., mean diameter along root (D_{m}), diameter at breakage (D_{b}), and stele diameter (d_{s}). In addition, this study rejected the UT tests in which the samples broken at clamps or slipped off from clamps, to ensure the data remained free from boundary effects (Giadrossich et al. 2017).

3D printing. In this study, two types of 3D printing technologies, Fused Filament Fabrication (FFF, Prusa i3 MK3s) and Stereolithography (SLA, Prusa SL1), were employed. FFF extrudes thermoplastic filaments layer by layer from a heated nozzle, while SLA uses a laser to cure photo-sensitive resin in layers. Based on a review of literature and the technical data from manufacturers, the materials selected for FFF include Acrylonitrile Butadiene Styrene (ABS, Spectrum), Polylactic Acid (PLA, Polymer), Polycaprolactone (PCL, 3D4Makers), and Thermoplastic Polyurethane (TPU, Polymer). For SLA, the selected material is tough resin (Prusa). The subsequent tensile

experiments were conducted using rod-like solid specimens with varying diameters of 0.75, 1.25, 1.75, and 3 mm. Hollow specimens had an outer diameter of 1.75 mm with inner diameter of 0.875 mm, as well as an outer diameter of 3 mm with inner diameters of 0.75, 1.5, and 2.25 mm.

Statistical analysis. The root characteristics we studied included root morphological and mechanical properties, as shown in Table 1. All data were tested for normality. Pearson's correlation coefficients were calculated for bivariate correlations. Relationships between root diameter and mechanical properties were fitted with power-law curves. Fitting parameters α and β were obtained using linear fitting of the log-log transformed data, which improved the homoscedasticity of the variance of the data, thus reducing statistical bias associated with power-law fitting methods. All statistical analyses were performed using IBM SPSS Statistics 29.0.1.1 (SPSS Inc., Chicago, USA).

Table 1. Notation and definition.

Symbol	Unit	Definition
SDR	-	Stele diameter ratio, i.e., d_s/D_b.
F_f	N	The applied loading causing root first fracture in tension.
$\sigma_{m,\,f}$	MPa	Tensile stress for root first fracture calculated based on D_m, i.e., $F/0.25\pi {D_m}^2$.
$\sigma_{b,\,f}$	MPa	Tensile stress for root first fracture calculated based on D_b, i.e., $F/0.25\pi {D_b}^2$.
$\sigma_{s,\,f}$	MPa	Tensile stress for root first fracture calculated based on d_s, i.e., $F/0.25\pi {d_s}^2$.
σ_f	MPa	σ_f is defined as a generalized notation to encompass $\sigma_{m,\,f}$, $\sigma_{b,\,f}$ and $\sigma_{s,\,f}$.
ε_f	-	Root tensile strain when the first fracture (as shown in Fig. 2a.) occurs.
$F_{5\%}$	N	The applied loading causing 5% tension strain of a root.
$\sigma_{m,\,5\%}$	MPa	Tensile stress for 5% tension strain by D_m, i.e., $F_{5\%}/0.25\pi {D_m}^2$.
$\sigma_{b,\,5\%}$	MPa	Tensile stress for 5% strain by D_b, i.e., $F_{5\%}/0.25\pi {D_b}^2$.
$\sigma_{s,\,5\%}$	MPa	Tensile stress for 5% strain by d_s, i.e., $F_{5\%}/0.25\pi {d_s}^2$.
$\sigma_{5\%}$	MPa	$\sigma_{5\%}$ is defined as a generalized notation to encompass $\sigma_{m,\,5\%}$, $\sigma_{b,\,5\%}$ and $\sigma_{s,\,5\%}$.
E_m	MPa	Modulus of elasticity by D_m; defined as the elastic zone of the slope of stress-strain curves.
E_b	MPa	Modulus of elasticity by D_b.

RESULTS

Tension failure of natural roots. In the study, there existed three types of typical stress-strain curves for roots subjected to uniaxial tension, as shown in the Fig. 1 (a). The probability was quantified as follows: Type I behaviour occurred in 39.1% of the cases, Type II in 30.4%, and Type III in 30.4%. Typically, one root has tortuosity, and produces a certain amount of initial stiffness, which will resist straightening, thus mobilizing a low level of tensile stress during the initial deformation stages. Subsequently, Type I roots showed distinct linear elasticity, while the elastic-plastic behaviour can be clearly recognized in Type II and III. In particular, Type III roots presented a multi-peak behaviour in the plastic phase. Fig. 1(b) illustrates the diameter distribution of different stress-strain behaviours. Based on the analysis of the first quartile, median, and third quartile values, the data revealed that roots with Type II behaviour tended to have larger diameters, indicating that the tensile behaviour of more mature roots is typically elastoplastic.

During tension, accumulative fractures of the outer tissue (epidermis and cortex) were observed prior to the ultimate breakage of roots (Fig. 2a). The phenomenon indicated that a

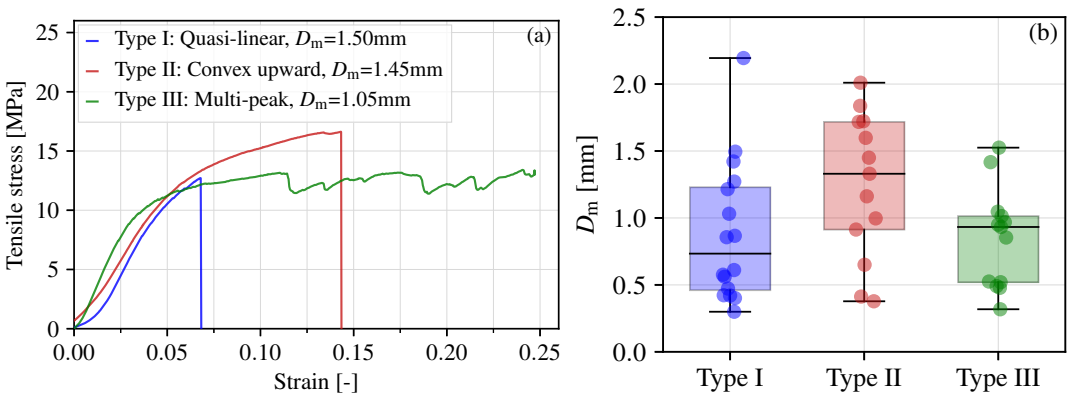

Figure 1. (a) Typical tensile stress-strain curves of three root samples with similar diameters; (b) Diameter distribution of different stress-strain behaviours.

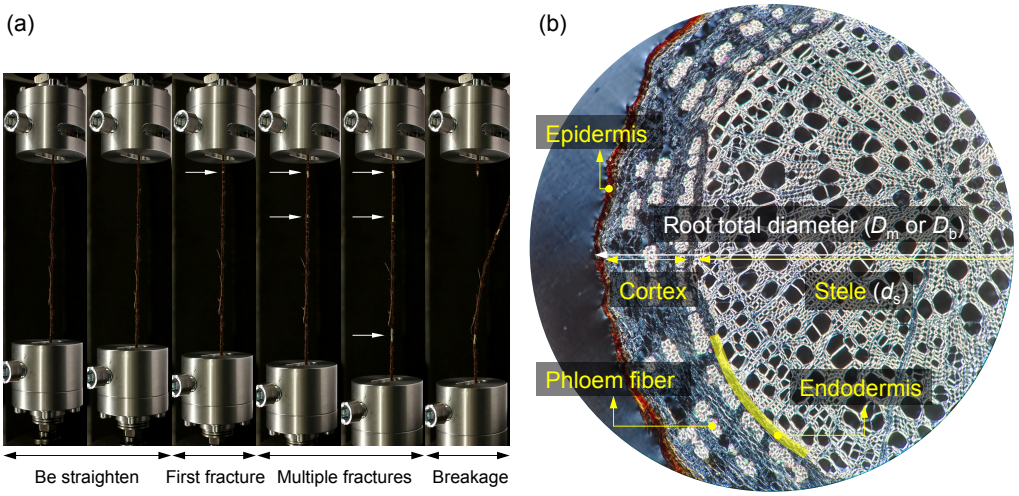

Figure 2. (a) Process of root breakage under tension; (b) Root microscopy of *S. purpurea* root.

root functioned as a composite structure rather than a single homogeneous material. Microscopic analysis of the root structure revealed that the outer tissue mainly consisted of the cortex, while the inner tissue was identified as the stele (Fig. 2b).

Tensile properties of natural roots. Figure 3 presents the results of Pearson correlation analysis for root morphological and mechanical parameters, indicating that SDR was moderately correlated with root diameter (D_m, D_b, and d_s), consistent with findings reported in the literature (Mao et al. 2018; Meijer et al. 2024). F_f exhibited a strong positive correlation with three diameter variables, and a moderate positive correlation with SDR. Additionally, a weak negative correlation was observed between $\sigma_{m,f}$ and D_m, as well as between $\sigma_{b,f}$ and D_b. SDR was found to be more correlated to σ_f, and E_m or E_b than D_m, D_b, and d_s. No significant relationship was found between ε_f and modulus of elasticity (E_m, E_b) with root diameter. However, a strongly positive correlation was observed between E_m and $\sigma_{m,f}$, as well as between E_b and $\sigma_{b,f}$.

Figure 4 shows the power regression of root tension properties and diameter. In addition to the tension properties at the initial fracture, root tension properties at a certain level of tension strain (e.g., 5%) were also evaluated. This study indicated that D_m, D_b and d_s were able to explain

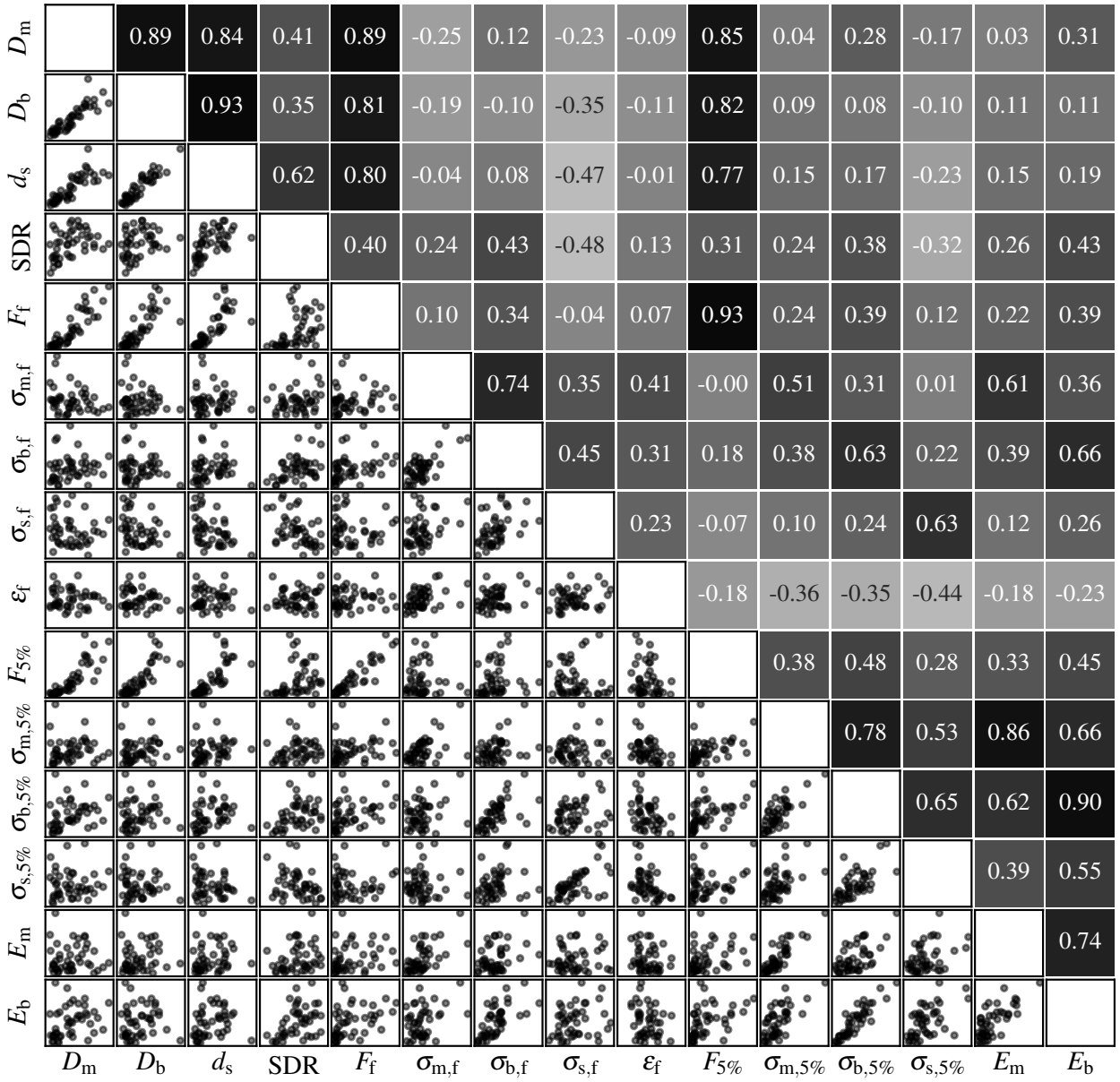

Figure 3. Pearson correlation analysis for root morphological and mechanical parameters.

a larger proportion of the observed variation in the F_f (Fig. 4a,b,c, Table 2). However, the power law could not well describe the relationship between $\sigma_{m,f}$ and D_m, as well as between $\sigma_{b,f}$ and D_b (Fig. 4e,f, Table 2). By contrast, stele diameter d_s could explain a larger proportion of the variation in the $\sigma_{s,f}$ (R^2 increased from 0.001 to 0.41 (Fig. 4g, Table 2)). The explained variation in $\sigma_{s,5\%}$ was increased substantially (0.02 to 0.17). In addition, $\sigma_{s,f}$ versus SDR and $\sigma_{s,5\%}$ versus SDR curves provided more accurate fits, with R^2 reaching 0.43 and 0.28, respectively (Fig. 4h,p, Table 2). This suggested that the SDR-based power regression captured the relationship more effectively.

In terms of *S. purpurea*, ε_f were consistently less than 25% (Fig. 5). Across all data, no distinct patterns were observed for ε_f as a function of D_m, D_b, d_s, and SDR. However, when clustering data based on different tensile stress-strain behaviours, it was found that the order of ε_f

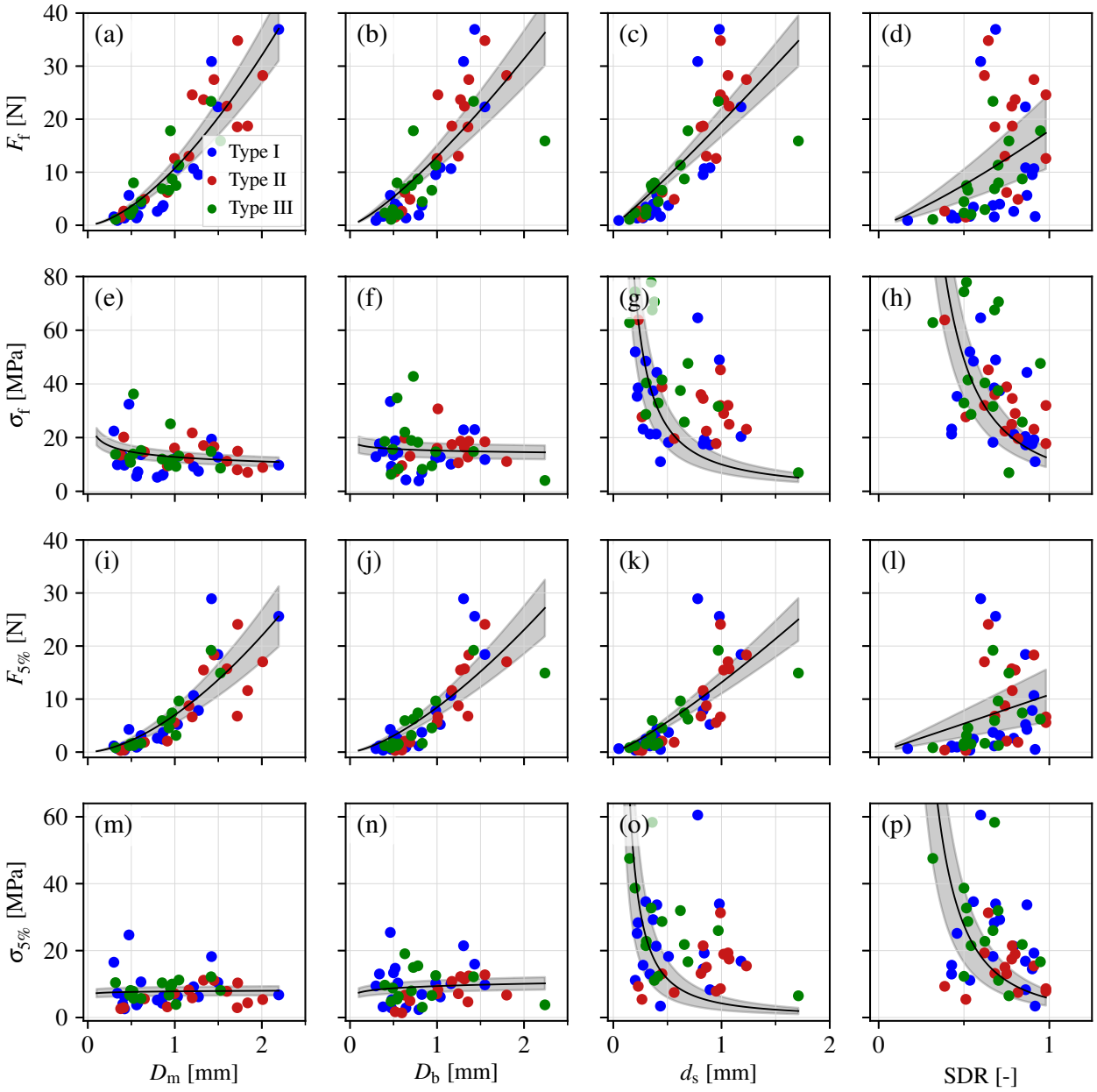

Figure 4. Measured and fitted root mechanical parameters. The power-law regression is shown by black solid lines, with lightly shaded black areas representing the 95% confidence interval.

followed the sequence: Type II > Type III > Type I. Type I roots exhibited the lowest ε_f due to undergoing only elastic phase without significant plastic deformation. In Type III roots, cortex-stele debonding made the cortex more prone to breakage during tension, resulting in a lower ε_f compared to Type II roots. This explains why ε_f was greater in Type II roots than in Type III roots.

Preliminary results of root analogues. The tensile testing results of the filament-based root analogues indicated that the stress-strain behaviour of PCL most closely resembled that of real willow roots (Fig. 6a). In contrast, both PLA and ABS exhibited significantly higher initial stiffness and ultimate tensile stress compared to natural roots, but their fracture strain is smaller

Table 2. Regression functions.

Dataset	Parameter	D_m [mm]			D_b [mm]			d_s [mm]			SDR [-]		
		α	β	R^2	α	β	R^2	α	β	R^2	α	β	R^2
All data	F_f [N]	9.27^{***}	1.83^{***}	0.85	10.5^{***}	1.95^{***}	0.76	17.74^{***}	1.41^{***}	0.80	15.93^{***}	2.01^{***}	0.37
	σ_f [MPa]	11.8^{***}	-0.16	0.04	13.34^{***}	-0.05	0.00	22.6^{***}	-0.59^{***}	0.41	19.69^{***}	-1.27^{***}	0.43
	$F_{5\%}$ [N]	5.5^{***}	2.11^{***}	0.84	6.3^{***}	2.22^{***}	0.73	11.01^{***}	1.55^{***}	0.71	9.29^{***}	2.08^{***}	0.30
	$\sigma_{5\%}$ [MPa]	6.99^{***}	0.12	0.02	8.04^{***}	0.21	0.03	11.74^{***}	-0.45^{**}	0.17	11.51^{***}	-1.19^{***}	0.28
	ε_f [-]	0.10^{***}	-0.01	0.00	0.10^{***}	0.01	0.00	0.10^{***}	0.05	0.01	0.11^{***}	0.16	0.02
Type 1	F_f [N]	7.82^{***}	1.82^{***}	0.84	9.40^{***}	1.97^{***}	0.76	13.65^{***}	1.29^{***}	0.72	8.75^{***}	1.49^{**}	0.29
	σ_f [MPa]	9.93^{***}	-0.180	0.04	11.97^{***}	-0.04	0.00	1.05^{***}	-0.72^{**}	0.45	1.02^{***}	-1.51^{***}	0.60
	$F_{5\%}$ [N]	5.80^{***}	2.10^{***}	0.81	7.07^{***}	2.23^{***}	0.73	10.27^{***}	1.40^{***}	0.64	6.06^{***}	1.54^{**}	0.23
	$\sigma_{5\%}$ [MPa]	7.37^{***}	0.10	0.01	9.02^{***}	0.23	0.03	0.95^{***}	-0.60^{*}	0.24	0.88^{***}	-1.46^{**}	0.43
	ε_f [-]	0.07^{***}	-0.25	0.14	0.07^{***}	-0.19	0.07	0.07^{***}	-0.07	0.02	0.07^{***}	-0.02	0.00
Type 2	F_f [N]	10.49^{***}	1.71^{***}	0.90	11.51^{***}	2.31^{***}	0.87	21.67^{***}	1.72^{***}	0.90	25.59^{***}	2.19^{*}	0.33
	σ_f [MPa]	13.40^{***}	-0.29	0.20	14.64^{***}	0.31	0.11	1.20^{***}	-0.28	0.18	1.13^{***}	-0.93^{**}	0.47
	$F_{5\%}$ [N]	4.19^{***}	2.50^{***}	0.90	4.80^{***}	3.39^{***}	0.88	12.21^{***}	2.54^{***}	0.92	15.90^{***}	3.29^{*}	0.35
	$\sigma_{5\%}$ [MPa]	5.36^{***}	0.49	0.26	6.20^{***}	1.32^{**}	0.54	1.01^{***}	0.55^{*}	0.35	0.97^{***}	0.18	0.01
	ε_f [-]	0.15^{***}	-0.29^{**}	0.46	0.15^{***}	-0.41^{**}	0.50	0.13^{***}	-0.23^{*}	0.29	0.14^{***}	-0.08	0.01
Type 3	F_f [N]	10.07^{***}	1.76^{***}	0.83	9.39^{***}	1.43^{**}	0.56	17.05^{***}	1.25^{***}	0.78	21.78^{***}	2.55^{***}	0.63
	σ_f [MPa]	12.82^{***}	-0.23	0.07	11.94^{***}	-0.57	0.17	1.12^{***}	-0.76^{**}	0.57	1.19^{***}	-0.83	0.13
	$F_{5\%}$ [N]	6.41^{***}	2.12^{***}	0.91	6.12^{***}	1.84^{***}	0.70	11.38^{***}	1.42^{***}	0.78	11.78^{***}	2.41^{**}	0.43
	$\sigma_{5\%}$ [MPa]	8.15^{***}	0.11	0.03	7.78^{***}	-0.16	0.02	0.98^{***}	-0.58^{*}	0.37	0.98^{***}	-0.96	0.20
	ε_f [-]	0.10^{***}	0.01	0.00	0.10^{***}	-0.19	0.07	0.10^{***}	-0.07	0.02	0.11^{***}	0.17	0.02

Significance: $^{***}(P \leq 0.001)$; $^{**}(0.001 < P \leq 0.01)$; $^{*}(0.01 < P \leq 0.05)$.

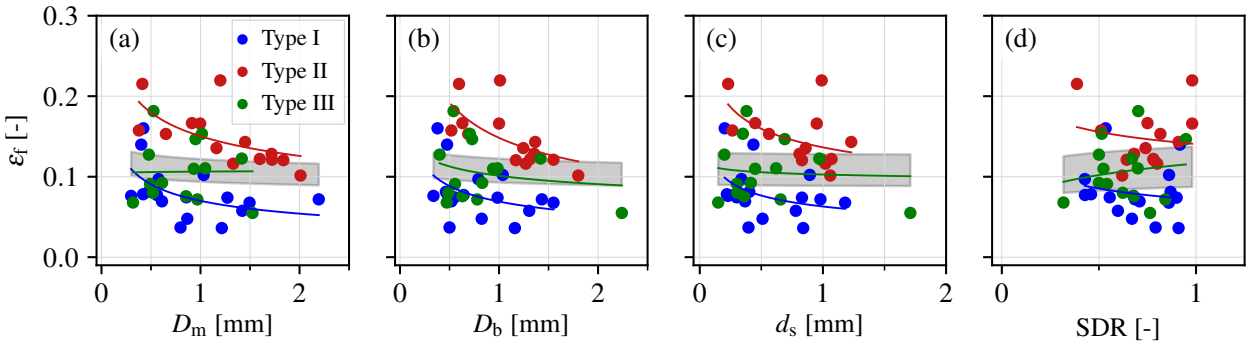

Figure 5. Root first fracture strain ε_f versus D_m, D_b, d_s, and SDR.

than that of natural roots. Although the ultimate tensile stress and fracture strain for TPU were not obtained, it was hypothesized that TPU would exhibit the opposite trend compared to PLA and ABS, namely, significantly lower initial stiffness and strength but much higher fracture strain. In comparison, resin-based analogues demonstrated substantial potential for accurately simulating the tensile behaviour of real willow roots.

Figure 6(b) compared the tensile parameters of root analogues with varying diameters and printing (i.e., solid and hollow) to those of *S. purpurea* roots. It was observed that both PCL and resin somewhat fell within the mechanical parameter range of natural roots. Notably, the fracture strain of PCL corresponded to the strain at the first significant drop in stress.

As previously discussed, roots could be considered a composite material consisting of cortex and stele. In the study, some hollow structures were printed to simulate the cortex, with future work

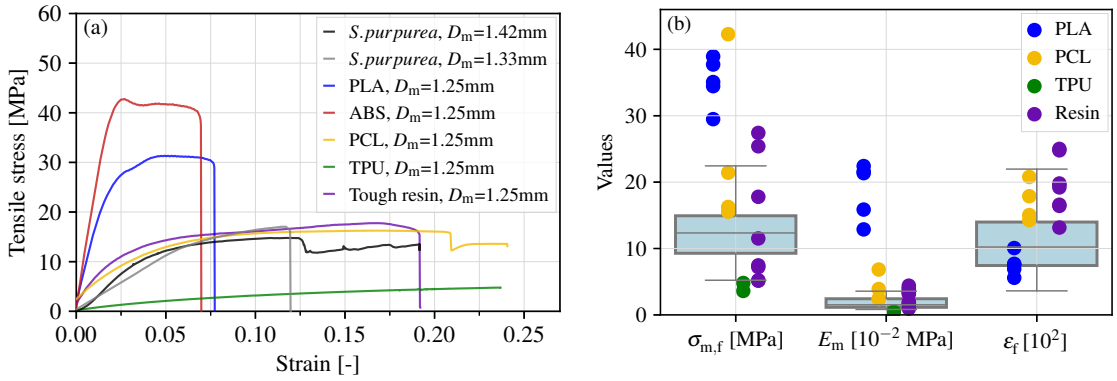

Figure 6. Comparison of (a) stress-strain behaviour and (b) mechanical parameters between real roots and root analogues. The boxplot presents the data of *S. purpurea*.

focusing on identifying suitable materials (e.g., grouting materials) to simulate the stele. As shown in Fig. 7, for resin, hollow printing reduced the initial stiffness and strength of the root analogues but had little effect on the fracture strain. For PCL, whether hollow or solid, the root analogues exhibited a sudden drop in stress to a stable value. Unlike resin, the hollow configuration did not reduce the initial stiffness and strength of PCL-based root analogues.

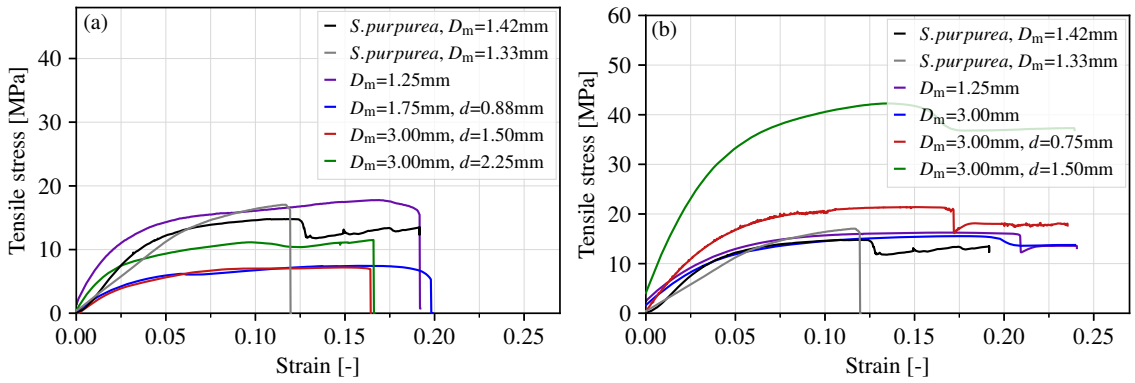

Figure 7. Tensile behaviour of hollow root analogues: (a) Tough resin and (b) PCL.

DISCUSSION

Throughout existing research, only several authors (Tosi 2007; Boldrin et al. 2018; Wu et al. 2024; Meijer et al. 2024) have presented the tensile stress-strain curves of roots. Most of these authors suggested roots showed the typical biphasic nature with both elastic and inelastic response (Boldrin et al. 2018; Wu et al. 2024), which was consistent with Type II behaviour in this study. However, this study revealed more diverse stress-strain behaviour of roots, which probably depended on the chemical composition and anatomical traits of roots. As a primary chemical component, high cellulose content is generally associated with increased rigidity and tensile strength, which can influence the overall mechanical behaviour of the root (Kamchoom et al. 2022).

The tensile stress-strain behaviour of roots in the plastic phase was likely influenced by the bonding strength between cortex and stele. Meijer et al. (Meijer et al. 2024) observed the instances

of debonding between cortex and stele in some tomographic images of maize roots. Specifically, if the debonding occurred, the breakage process began in the cortex, leading to stress redistribution. Then multiple cortex breakage occurred until the stele eventually breaking. This results in Type III stress-strain behavior, explaining stress fluctuations during the plastic phase. Without the debonding between cortex and stele, root would exhibit Type II behaviour, with simultaneous breakage in both the cortex and stele.

The increase in F_f as D_m or D_b increased in the study aligns with most of the literature (Li et al. 2023). In addition, both linear and power law regression indicated a stronger relationship between D_m with F_f and $F_{5\%}$, compared to D_b (Fig. 3, Table 2). Previous studies observed a negative power relationship between σ_f and root diameter (D_m or D_b) (Li et al. 2023). However, D_m or D_b as the sole predictor of root strength has recently become controversial, as root cortex played a minor role compared to the stele, which is the primary load-bearing tissue under tension (Meijer et al. 2024). In this study, D_m or D_b were similarly found to be ineffective indicators of the variation encountered in σ_f and $\sigma_{5\%}$. Instead, d_s and SDR were better predictors of σ_f and $\sigma_{5\%}$, further supporting the correlation between root mechanics and root anatomical structure.

In recent years, ABS and TPU filaments used in Fused Filament Fabrication (FFF) have gained popularity as materials for root analogues (Liang et al. 2017; Kim et al. 2024). However, for the willow roots tested in this study, ABS did not accurately represent the tensile strength and Young's modulus, while TPU exhibited a failure strain significantly greater than that of natural roots. By comparison, resin-printed and PLA-printed root analogues more closely resembled natural willow roots in terms of their uniaxial tension properties. Among these, resin prints demonstrated superior accuracy over PLA-based prints. This accuracy is crucial when complex root architecture is involved.

CONCLUSION

The conclusion obtained in this study are summarized as follows: (1) In the tensile tests, the three typical stress-strain curves were recognized, and the variability of root behaviour was caused by a combination of multiple fractures in the cortex and partial debonding of the stele–cortex interface. (2) The strength and stiffness of stele and cortex were found to be substantially different. The stele primarily bears the load and elongation, while cortex contributes to the overall structural integrity. It was therefore imperative to conceptualize the single root as a composite structure consisting of two distinct materials, rather than as a uniform, homogeneous material. (3) Compared to root diameter (D_m or D_b), root stele should be more responsible for root tensile properties. (4) Our preliminary tests indicated that resin prints by SLA could give repeatable and representative uniaxial tensile properties for natural *Salix purpurea*. SLA technique is therefore promising in the parametric (e.g., root area ratio, root length, branching pattern, tortuosity, etc.) studies of soil-root interaction.

ACKNOWLEDGMENT

The authors want to thank Mr. Schlüter (Federal Waterways Engineering and Research Institute) for his invaluable assistance in sampling the plant roots essential for my experiments. The authors also extend sincere thanks to Mr. Busch and Mr. von Dollen, from KIT's Institute of Applied Geosciences for their crucial support in sample preparation for root microscopy.

REFERENCES

Ali, F., Osman, R., and Kamil, SSSM. (2013). "The influences of root branching patterns on pullout resistance." *EJGE*, 18, 3967–3977.

Boldrin, D., Leung, A. K., and Bengough, A. G. (2018). "Effects of root dehydration on biomechanical properties of woody roots of Ulex europaeus." *Plant and Soil*, 431(1-2), 347–369.

Chen, C., Wu, L., and Harbottle, M. (2019). "Influence of biopolymer gel-coated fibres on sand reinforcement as a model of plant root behaviour." *Plant and Soil*, 438(1-2), 361–375.

Fleischer, P., Gesing, C., and Stelzer, O. (2021). "Technisch-biologische ufersicherungen – bemessungskonzept für die ingenieurpraxis an binnenwasserstraßen." *geotechnik*, 44(3), 178–190.

Giadrossich, F., Schwarz, M., Cohen, D., Cislaghi, A., Vergani, C., Hubble, T., Phillips, C., and Stokes, A. (2017). "Methods to measure the mechanical behaviour of tree roots: A review." *Ecological Engineering*, 109(part B), 256–271.

Kamchoom, V., Leung, A. K., Boldrin, D., Sakolpanya, T., Wu, Z., and Likitlersuang, S. (2022). "Shearing behaviour of vegetated soils with growing and decaying roots." *Canadian Geotechnical Journal*, 59(12), 2067–2084.

Kim, Y.-A., Burrall, M., Jeon, M.-K., DeJong, J. T., Martinez, A., and Kwon, T.-H. (2024). "Pullout behavior of tree root-inspired anchors: Development of root architecture models and centrifuge tests." *Acta Geotechnica*, 19(3), 1211–1229.

Li, S., Wang, Z., and Stutz, H. H. (2023). "State-of-the-art review on plant-based solutions for soil improvement." *Biogeotechnics*, 1(3), 100035.

Liang, T., Knappett, J. A., Bengough, A. G., and Ke, Y. X. (2017). "Small-scale modelling of plant root systems using 3D printing, with applications to investigate the role of vegetation on earthquake-induced landslides." *Landslides*, 14(5), 1747–1765.

Mao, Z., Wang, Y., McCormack, M. L., Rowe, N., Deng, X., Yang, X., Xia, S., Nespoulous, J., Sidle, R. C., Guo, D., and Stokes, A. (2018). "Mechanical traits of fine roots as a function of topology and anatomy." *Annals of Botany*, 122(7), 1103–1116.

Martinez, A., Dejong, J., Akin, I., and et al. (2022). "Bio-inspired geotechnical engineering: Principles, current work, opportunities and challenges." *Géotechnique*, 72(8), 687–705.

Meijer, G. J., Lynch, J. P., Chimungu, J. G., and Loades, K. W. (2024). "Root anatomy and biomechanical properties: improving predictions through root cortical and stele properties." *Plant and Soil* (Published online).

Mickovski, S. B., Bengough, A. G., Bransby, M. F., Davies, M. C. R., Hallett, P. D., and Sonnenberg, R. (2007). "Material stiffness, branching pattern and soil matric potential affect the pullout resistance of model root systems." *European Journal of Soil Science*, 58(6), 1471–1481.

Schwarz, M., Cohen, D., and Or, D. (2011). "Pullout tests of root analogs and natural root bundles in soil: Experiments and modeling." *Journal of Geophysical Research: Earth Surface*, 116(F2).

Sonnenberg, R., Bransby, M., Bengough, A., Hallett, P., and Davies, M. (2012). "Centrifuge modelling of soil slopes containing model plant roots." *Canadian Geotechnical Journal*, 49(1), 1–17.

Tosi, M. (2007). "Root tensile strength relationships and their slope stability implications of three shrub species in the northern apennines (italy)." *Geomorphology*, 87(4), 268–283.

Wu, T. H., McOmber, R. M., Erb, R. T., and Beal, P. E. (1988). "Study of Soil-Root Interaction." *Journal of Geotechnical Engineering*, 114(12), 1351–1375.

Wu, Z., Leung, A. K., and Boldrin, D. (2024). "Mechanical responses of chrysopogon zizanioides roots under cyclic loading conditions." *Plant and Soil*, 494(1-2), 437–459.